Intraseasonal Convective Perturbations related to the Seasonal March of the Indo-Pacific Monsoons

H. Bellenger and J.P. Duvel

Laboratoire de Météorologie Dynamique, ENS, Paris, France

13 April 2006

Revised 9 October 2006

Corresponding author address:
Dr. Jean-Philippe Duvel,
Laboratoire de Météorologie Dynamique,
Ecole Normale Supérieure,
24 rue Lhomond, F-75231
Paris Cedex 05, France.
E-mail: jpduvel@lmd.ens.fr

Abstract

The seasonal evolution of the 20-90 day intraseasonal variability (ISV) of the convection in the Indo-Pacific region presents intriguing features related to monsoon dynamics: (i) a sharp ISV maxima in May for the southern Bay of Bengal and in June for the Eastern Arabian sea; (ii) maximum ISV over the West Pacific in July-September when the ISV over northern Indian Ocean is weaker; (iii) persistent ISV north of Australia from December to March; (iv) weak ISV over continental regions. The source of these behaviours is investigated from time series of satellite observations, meteorological re-analysis and from an ocean mixed layer depth (MLD) climatology. For the northern Indian Ocean, sharp ISV maxima in May and June, when the MLD is still small (~20-30m), are related to an abrupt surface cooling associated to the setting of the monsoon low-level jet. The ISV of the convection is smaller over these regions during July-September when the MLD is deepened (~60-70m) by the monsoon low-level wind forcing. At this time, the low-level wind is weak over the West Pacific, the MLD is small and the amplitude of the ISV remains large. North of Australia, and also over the south equatorial Indian Ocean, there is no particular reinforcement of the ISV near the onset. A weak low-level jet and a small MLD prevail during the whole monsoon season in good agreement with a more uniform ISV. These results support the hypothesis that a moderately shallow (~20-30m) ocean mixed layer is important for maintaining locally the ISV of the convection, when the conditions (e.g. SST, large-scale circulation) for such ISV to exist are satisfied. The seasonal variability of the MLD, related in part to the monsoon low-level jet variability over the tropical oceans, gives thus a link between the seasonal march of monsoon circulations and the seasonal evolution of the ISV of the convection. This has implications for a better understanding of the origin of the ISV and for the predictability of its amplitude, especially near the monsoon onset date.

1. Introduction

The 20-90 day intraseasonal variability (ISV) of the tropical deep convection strongly perturbs the seasonal cycle in the Indo-Pacific tropical region, giving in particular breaks and active phases for both Asian and Australian monsoons. The analysis of the link between the ISV and the seasonal evolution of the monsoon is thus important to improve our knowledge of the seasonal march of the monsoon. In particular, this is necessary to better understand the link between ISV and monsoon onsets that gives element of predictability for the rain distribution at the beginning of the monsoon season. Hendon and Liebmann (1990) showed that the onset of the Australian monsoon indeed coincides with the first occurrence of 40-50 day eastward propagating convective events. Over the Bay of Bengal, the double monsoon onset (Flatau et al, 2001) linked to the seasonal cycle also corresponds to an intraseasonal perturbation of the convection. By looking at a multiyear average of the OLR seasonal cycle, Wang and Xu (1997) shows evidence of "climatological intraseasonal oscillations" in the East Asian Monsoon. Ho and Wang (2002) distinguished the slow seasonal variation from a "fast annual cycle" that can be considered as transitions at the intraseasonal time-scales. More recently, Zhang and Dong (2004), rather looking at the influence of the mean background state on a specific Madden Julian Oscillation (MJO) index, showed that the MJO amplitude is maximal around 10° of latitude during the summer season of each Hemisphere. All these studies, with various approaches over different regions, show a climatological relation between the seasonal evolution of the monsoon circulation and different characteristics (amplitude, timing in regard to the onset) of the ISV of the convection. In this context, the ISV should not be considered only as a random feature superimposed on a more predictable large-scale persistent component of the monsoon (Krishnamurthy and Shukla, 2000). Indeed, the ISV is also possibly an intrinsic part of the monsoon seasonal progression.

The coupling with the ocean could play a fundamental role in this link between the monsoon and the ISV. Indeed, recent observations showed that large-scale intraseasonal events of the tropical deep convection are associated to strong intraseasonal perturbations of the SST in the Indian Ocean (Sengupta and Ravichandran, 2001; Harrison and Vecchi, 2001; Vecchi and Harrison, 2002; Duvel et al, 2004). Modelling studies also suggest that air-sea interactions could play an important role in the ISV (e.g. Waliser et al. 1999; Inness and Slingo 2003; Maloney and Sobel 2004). This interaction between the SST and the convection at the intraseasonal time scale is based on the perturbation of the surface fluxes by the atmospheric

convective activity. In convectively suppressed conditions, the ocean surface warms up because of the stronger solar surface flux. This effect is larger under low wind conditions (reduced surface turbulent heat fluxes and formation of ocean warm layers). For a larger SST, the boundary layer is warmer and moister and the convective instability is potentially increased (see Stephens et al, 2004). During a convective event, enhanced evaporation and reduced solar flux related to the convective activity cool the surface and thus tend to reduce the convective instability. For such a process, the amplitude of the resulting ISV of the SST will depend on the amplitude of the surface turbulent and radiative flux perturbations related to the convection and on the local ocean Mixed Layer Depth (MLD). Results reported in Duvel and Vialard (2006) confirm that, despite the role of other factors (e.g. ocean warm layers, upwelling), the surface fluxes and the MLD remain the main factors governing the intraseasonal perturbations of the SST. A thin MLD is necessary to have a large (i.e. a few K) warming and cooling at the intraseasonal time-scale. However, the MLD has also to be thick enough to contain sufficient energy to maintain the convective instability for around 10-15 days, and this despite an enhanced surface latent heat flux and a reduced solar input. This process has been already theoretically studied by Sobel and Gildor (2003) and tested by Maloney and Sobel (2004) using numerical experiments involving a simplified model and an atmospheric GCM coupled to a slab ocean. They showed that the ISV of the convection during NH winter is maximal for a MLD around 20-30 meters.

One may thus expect, and this will be inspected in this paper, that the ISV pattern has a seasonal evolution partly driven by the seasonal distribution of the MLD. In addition, if one considers that the seasonal evolution of the MLD in the tropics is partly forced by the monsoon low-level wind, the MLD gives a possible link between the seasonal march of the monsoon circulation and the seasonal evolution of the ISV of the convection. This point is particularly interesting to understand the link between the monsoon onset and the ISV, since the setting of the low-level monsoon jet will rapidly deepen and cool the ocean mixed layer. This is also interesting because it gives some elements of predictability of the amplitude of the ISV if one considers the more predictable seasonal evolution of the low-level circulation.

This analysis of the role of the MLD in the ISV of the convection does not imply that the coupling with the surface is the only mechanism enhancing the convective instability at intraseasonal time-scales. This coupling with the surface has to be complemented by other processes that may also trigger or amplify the ISV of the convection. Large-scale processes must be considered, such as subsidence that can inhibit the convection over warming water,

giving a larger warming over a more extended region that may later favour a large-scale convective event. Also, the coupling between convective and dynamical intraseasonal perturbations obviously plays a critical role in the physics of the ISV over a given basin. For example, over the northern Indian Ocean region during the NH summer, Lawrence and Webster (2002) showed that the northward moving portion of convection is forced by surface frictional convergence into the low-pressure center of the Rossby cell that is excited by equatorial perturbation of the convection. These authors also noted that a warm SST is necessary for this process to occur. In this context, the impact of the MLD on such a coupled (dynamics and convection) perturbations may be understood as an additional coupling with surface conditions. The hypothesis is that the surface processes can amplify the convective perturbation linked to the dynamical perturbation, giving on the average more ISV of the convection over the considered basin.

The relation between the monsoon dynamics, surface conditions and the ISV is inspected from a climatological point of view by analysing: (i) the average seasonal evolutions of surface parameters (rainfall, SST and MLD) and low-level wind and, (ii) the corresponding seasonal evolution of the ISV characteristics. The paper is organized as follows. In section 2, data and analysis approaches are described. Section 3 discusses monthly evolution of the ISV distribution over the Indo-Pacific area. In order to further explore the origin of this distribution, seven monsoon regions are selected because of their specific seasonal cycle of the ISV. The selection of these seven regions is also based on the relative homogeneity of the average seasonal evolution of the OLR. In section 4, points (i) and (ii) above are analysed in detail for these seven monsoon regions. The seasonal distribution of the strongest intraseasonal events and composites of these strongest ISV events occurring close to the monsoon onset are also analysed. Summary and discussions are reported in section 5.

2. Data and analysis method

Daily-mean NOAA OLR on 2.5° regions from January 1979 to December 2004 is used as a proxy for the tropical deep convection. The 850 hPa wind speed from NCEP reanalysis and SST from the Reynolds and Smith (1994) algorithm (daily interpolated) are also used at the same spatiotemporal resolution. We also use the monthly-mean MLD dataset of de Boyer Montégut et al (2004). In this dataset the MLD is estimated from temperature profiles measurements taken from 1941 to 2002. The MLD is defined as the depth at which temperature is 0.2K cooler compared to the temperature at a depth of 10 meters. In the Indo-

Pacific region, the number of profiles appears to be sufficient to warrant the reliability of the climatology. However, the formation of barrier layers due to strong precipitations or to large fresh water run-off along the coast could give smaller MLD using a density instead of a temperature criterion. On the basis of a few available temperature and salinity profiles de Boyer Montégut et al (2004) give an estimate of the differences between the two approaches. In the Indo-Pacific region, this difference is maximal (reaching 30m) in some regions of the Bay of Bengal during winter months. This difference decreases to 10m in April-June and is more generally negligible during summer months for most of our regions of interest. As reported in Shenoi et al (2002), the barrier layer near the North-West boundary of the Bay of Bengal is however very persistent during the boreal summer and could lead locally to an overestimated MLD in the de Boyer Montégut climatology. This will be further commented in the following sections.

The ISV considered here is simply the variance of the time series of each 2.5° region in the 20 to 90 day band. Since the aim is to extract the average seasonal evolution of the ISV, the mathematical processing must be able to give a continuous estimation of the ISV variance (like a wavelet analysis but for a single frequency band). To this end, a complex demodulation (e.g. Julian, 1971) of the time-series is performed following:

$$\tilde{X}_f(t) = \frac{1}{N} \sum_{k=k_1}^{k_2} \left(\sum_{n=1}^{N} X(n) e^{-2i\pi k \frac{n}{N}} \right) e^{2i\pi t \frac{k}{N}}$$

Where k_1 and k_2 are harmonics corresponding to period of 20 and 90 days, t and n are time in day, X(n) is the original daily time series and $\tilde{X}_f(t)$ is the complex demodulated signal. The module $\left|\tilde{X}_f(t)\right|$ gives the evolution of the 20-90 day band variance and its real part $\Re\left(\tilde{X}_f(t)\right)$ is the filtered signal. This method is applied for OLR, SST and wind time series. The ISV is thus defined here by regional spectral characteristics with no *a priori* on the large-scale organisation of the perturbations (for example the eastward propagation for the MJO). This kind of analysis may be done providing that any strong convective intraseasonal event detected at the regional (i.e. 2.5°) scale corresponds to a large-scale organized event. This is generally true because of the relation between the time scale and the spatial scale of the convective perturbations and this is confirmed by the inspection of the patterns of individual intraseasonal events extracted by the Local Mode Analysis (Goulet and Duvel, 2000; Duvel and Vialard, 2006). In the following, we will link the occurrence and the amplitude of intraseasonal convective events to local MLD and SST conditions over large (~2000km x

2000km) regions. These events may be triggered locally or by a remote forcing. This is in agreement with the study of Annamalai and Sperber (2005) who consider the large-scale dynamical response related to regional heat sources and sinks and the impact on remote regions.

Since we are interested in the relation between the average seasonal evolution of the convective activity and the ISV, we will also have to define region with relatively homogeneous rainfall seasonal cycle. To this end, a simple regional index is computed using the daily OLR seasonal cycle averaged from years 1979 to 2004. For each 2.5° region, this OLR time series is used to determine the date of the strongest negative derivative that is expected to correspond to the date of the regional rainfall onset. If one considers that the monsoon onset corresponds to the setting of a large-scale circulation, this date should not be considered *stricto sensu* as a monsoon onset date (while this will be the case for some regions, as shown below). This derivative ($Wm^{-2}pentad^{-1}$) is estimated by the pentad-mean OLR difference between ±3 pentads (i.e. 30 days) relative to the considered day. For each 2.5° region, this approach define an "Average Rainfall Onset Date" (AROD) and an index of the abruptness of this rainfall onset called hereinafter the Average Rainfall Onset Intensity (AROI). An abrupt decrease in the average OLR signal means that there is a large and reproducible OLR decrease (i.e. rainfall onsets for this region occur close to a given calendar day each year) linked to the monsoon seasonal evolution. A threshold of -5 $Wm^{-2}pentad^{-1}$ is chosen because it well delineates the main monsoon area. Then, seven monsoon regions (represented on figure 2) with a relatively homogeneous AROD are selected to study in more detail the link between the ISV and the seasonal cycle.

In order to determine the distribution of intraseasonal events along the monsoon season, we identify the strongest intraseasonal events by applying a threshold of 40 Wm^{-2} in the difference between the maximum and the following minimum in $\Re(\tilde{X}_f(t))$ for OLR time series averaged over each of the seven selected regions. This threshold roughly corresponds to the average value of this difference augmented by one standard deviation. Depending on region, the number of strong events is between 32 (Northeast India) and 94 (South China Sea) for the 25-year period (Table 1). The average period of these intraseasonal events varies between 29 and 35 days with a standard deviation of about 7 days. By analogy with the definition of the AROD, the date attributed to these intraseasonal convective events is defined considering the decreasing phase in the filtered OLR signal $\Re(\tilde{X}_f(t))$ (the inflection point). An emphasis will be put on the distribution of these strongest events near the AROD. The aim

is to examine if these strong convective ISV events are linked to the monsoon low-level jet onset. In such a case, the abrupt and then persistent increase of the surface wind due to the low-level monsoon jet could deepen the ocean mixed layer and thus inhibits durably the ISV of the convection. This may also lead to a persistent decrease of the SST that will inhibit the convection itself. To study these processes, we will construct a composite of the strongest intraseasonal events occurring near the AROD. An event for a given year is considered only if it occurs less than 4 pentads from to the AROD. The number of events retained for the composite is only 12 for Northwestern Pacific Ocean and Northeast India but approaches one by year (20 and 21) for the Bay of Bengal and the Arabian Sea (Table 1).

3. Average seasonal cycle and the intraseasonal variability

As expected, (e.g. Goulet and Duvel, 2000; Zhang and Dong, 2004) the seasonal cycle of the ISV of the convection (Fig.1) follows the seasonal migration of the ITCZ. The maximum ISV of the convection is located over oceanic regions and generally off the equator, sometimes up to 15° of latitude. The only noticeable exception is the eastern equatorial Indian Ocean for which there is a continuous and moderate ISV all along the year, explaining why this region appears as the main ISV region if one considers the annual average. This is however not true on a monthly basis. From December to April, the ISV extends south of the equator from the Indian Ocean to the central Pacific Ocean, with maximum values North of Australia. From May to November, the ISV is more confined south of the Asian Continent with strong regional and temporal variability from one month to another. This variability of the ISV amplitude during NH summer has already been noticed in Kemball-Cook and Wang (2001) and is presented here for each month. Over the Bay of Bengal and the Arabian Sea there are sharp maxima in the ISV amplitude corresponding respectively to a bogus onset (Flatau et al, 2001) in May and to the onset of the Indian monsoon (Fasullo and Webster, 2003) in June (Fig.1). During the core of the monsoon season from July to September, the ISV of the OLR is weaker over northern Indian Ocean region while the ISV of the wind remains strong around 15°N. The Bay of Bengal also experiences a reinforcement of the ISV at the end of the monsoon in October and November. As already shown in Ho and Wang (2002), the maximum ISV for both OLR and wind is observed in August over the northwestern Pacific Ocean.

Maximum ISV for 850 hPa wind and OLR are not systematically collocated on figure 1. This is not surprising since the low-level wind response to diabatic heating due to deep convection will generally maximize outside the heating region (Gill, 1980). This will in particular

increase westerly wind to the west of the heating region. Note that for eastward moving perturbations, e.g. for NH winter near the equator, longitudinal shift that appear between two parameters for a particular phase of the ISV events is smoothed out in average amplitude maps. This westward extension of the wind ISV in regard to the OLR ISV is however particularly noticeable in August, when strong wind ISV over the northern Indian Ocean corresponds to enhanced OLR ISV over the northwestern Pacific Ocean. Such a remote dynamical response was already commented in Joseph and Sijikumar (2004). Also, Annamalai and Sperber (2005) simulated such a low-level wind response over the northern Indian Ocean due to warm surface and convectively induced diabatic heating over the northwestern Pacific. For our purpose, it is interesting to notice that the local or remote response of the low-level wind to the convective ISV may have an impact on the deepening of the ocean mixed layer. For a dominant westerly wind, such as monsoon low-level jet in the summer hemisphere, the module of the wind will be maximal during the convective events occurring further east. This may trigger or maintain a deepening of the ocean mixed layer due to low-level wind strengthening that will later inhibit the ISV of the convection over the corresponding region.

Figure 1 shows a strong reinforcement of the ISV over for the Bay of Bengal and the Arabian Sea during or just before the Indian monsoon onset in May and June. This apparent link between the monsoon onset and the ISV will be studied in detail for selected monsoon regions in the next section. These regions are selected based on the homogeneity of the distribution of the AROD and the AROI introduced in section 2. This distribution (Fig.2) well depicts the location of the main monsoon regions and is in good agreement with the results reported in Wang and Ho (2002) or Wang and Ding (2006). The monsoon index over the southwestern Pacific, weak for these two studies, is even weaker in our case and we will then not consider this region. Western and central Indian Ocean regions are identified as monsoon regions with the AROI threshold of -5 $Wm^{-2}pentad^{-1}$. These regions can indeed be considered as monsoon regions because the enhanced convection during NH winter corresponds to a large-scale cross equatorial circulation associated with a westerly low-level jet south of the equator. Based on the AROI, the homogeneity of the AROD and the seasonal evolution of the ISV (Fig.1), seven monsoon regions are defined (Fig.2).

4. Regional seasonal evolutions

The regional seasonal evolution of OLR, surface temperature and low-level wind and their ISV are represented together with the seasonal evolution of the MLD in figure 3. For the seven selected regions, the maximum SST is attained at or just before the AROD (Fig.3a), showing the regulating effect of the monsoonal convective activity on the surface temperature. As expected, the ISV of the OLR is strong only after the AROD. It is worth noting however that the ISV of the wind is also strong only after the AROD confirming that the coupling with the convection is a necessary condition (at least for these monsoon regions) to develop a large dynamical ISV. The impact of the MLD on the ISV of the convection thus makes sense only during the monsoon season after the AROD. Because of the expected impact of monsoon low-level jet on the surface wind stress, the MLD is well related to the 850 hPa wind during local summer months (Fig.3b). This is especially striking for northern Indian Ocean regions where the MLD increases greatly after the setting of the monsoon circulation. Over the Arabian Sea and the Northwestern Pacific Ocean during local winter months, the observed deepening of the MLD under relatively weak low-level wind may be attributed mainly to oceanic convection. Over the West Indian Ocean region, both low-level wind and MLD are maximal during NH summer due to the strong influence of the south-easterly jet related to the Indian summer monsoon.

Northern Indian Ocean and the Indian Monsoon

The regional distribution of the AROD (Fig.2 and 3a) well depicts the seasonal progression of the convective instability, with a rainfall onset over the southern Bay of Bengal in May and over the Arabian Sea in June. Northern India is, as expected, the latest region where the convection is triggered (Table 1). The SST decreases clearly after the AROD for the Arabian Sea and the Bay of Bengal (Fig.3a), giving a secondary SST minimum in the heart of the summer. This also corresponds to a dramatic increase of the MLD related to the setting of the low level monsoon jet. For these two regions, strong intraseasonal events clearly occur more often near the AROD (Fig.3d), giving maximal average ISV for OLR and SST (Fig.3c). This corresponds to period for which the MLD is about 30 meters on a climatological basis (Fig.3b). The ISV of both SST and OLR decreases in the heart of the monsoon as the MLD deepens to reach 70 meters in the Arabian Sea and 50 meters in the Bay of Bengal in association with the increase of low-level wind speed. As noted in section 2, this MLD could be overestimated in the Northwestern Bay of Bengal because of the formation of barrier layer

that are not taken into account in the climatology. However, this effect is small here because of the small weight of these northwestern regions on our large Bay of Bengal region. Note that the ISV of the SST is also certainly underestimated in the Reynolds dataset (Sengupta and Ravichandran, 2001; Duvel and Vialard, 2006). A secondary maximum of the ISV is reached during the autumn in association with a shallower MLD of about 30 meters in both basins. The reduction of the ISV of the convection in the core of the monsoon is also evident over continental India, while the ISV of wind and land surface temperature (diagnostic parameter in the re-analyses) are maximal. As suggested in figure 1, this maximum ISV of the wind over continental India could be due to the ISV of the convection that is maximal in July and August further east. Over the continent, there is no evident physical source explaining the reduction of the ISV of the convection in the core of the monsoon season (minimum OLR on Fig.3a). However, it is interesting to note that the first ISV maximum near the rainfall onset is in phase with the maximum over the Arabian Sea and that the ISV maximum in autumn corresponds to maxima over the Arabian Sea and the Bay of Bengal. This suggests that the amplitude of the ISV over India is partly driven by the basin-scale convective perturbation over surrounding oceanic regions.

There is clearly a group of strong intraseasonal events around the AROD for the three regions (Fig.4). In addition, for the Arabian Sea and Northeast India, these events near the AROD are among the strongest events for the whole monsoon season. For the Bay of Bengal there are two groups of strong events in May (onset) and November. For ISV events near the AROD (open circle in fig 4), a composite (see section 2) is performed for the three parameters (OLR, SST and low-level wind). The composite is just performed by averaging raw time series for each pentad around a reference date that corresponds to the decreasing phase of the filtered OLR time series.

Over the Arabian Sea, the wind composite increases by about $10ms^{-1}$ during the intraseasonal event (Fig.5). This is consistent with the average seasonal evolution of the wind relative to the AROD (Fig.3b) and this shows that the considered intraseasonal events indeed correspond to the setting up of the low-level monsoon jet. The SST is maximal during the convective development phase and then decreases continuously because of the low-level wind forcing. The next OLR maximum is attained 15 days after the minimum with an increase of more than $40Wm^{-2}$. This is remarkable since the composite of the 20 events (Table 1) is performed on the raw pentad mean signal. The resulting period of about 30 days is in good agreement with the average period of 33 days found considering the 68 strong events over this region (Table

1). Over the Bay of Bengal, the OLR remains relatively small after the rainfall onset and the average convective break in the composite is of weaker amplitude. Here, the composite intraseasonal event also corresponds to the setting of the low-level jet and to a decrease of the SST. The amplitudes are however smaller compared to the Arabian Sea, in good agreement with the average seasonal evolution (Fig.3a and 3b). Over Northeast India, this convective break is hardly visible showing the more variable durations of this first convective intraseasonal event from one year to another. For some years the rainfall onset over India is rather followed by short time-scales fluctuations related to the synoptic variability than by a break at intraseasonal time scale (not shown). The strength of the wind is only weakly perturbed by the intraseasonal event (Fig.5).

Northwestern Pacific Ocean and the East Asian Monsoon

The convection is triggered in May over the South China Sea, then in June for regions located immediately southeast and in July over the Northwestern Pacific Ocean (Fig.2). After the rainfall onset, the SST remains nearly constant over these regions (Fig.3a). The ISV of the convection is large during the core of the monsoon season and is associated to a persistent ISV of the SST (Fig.3c). The MLD stays indeed rather shallow throughout the season for these regions, in association with a moderate low-level wind. Over the Northwestern Pacific Ocean, the ISV of the wind is weak despite the relatively strong ISV of the OLR. This agrees with the hypothesis that the large-scale wind response is larger primarily to the southwest for a convective perturbation located north of the equator (Gill 1980; Annamalai and Sperber 2005).

The number of strong intraseasonal events is not particularly large near the AROD for these two regions (Fig.3d). There is a relatively even distribution of these strong intraseasonal events between May and November over the South China Sea and from July to November over the Northwestern Pacific Ocean. Interestingly, the AROD over the Northwestern Pacific Ocean corresponds to a reinforcement of the amplitude of intraseasonal events over the South China Sea region (Fig.3c and Fig.4). Considering the composite of the events occurring near the AROD, the oscillation of the OLR is marked (Fig.5) with an average period of the first intraseasonal event of about 20-30 days. There is a small increase of the low-level wind for the South China Sea region corresponding to the setting of a weak low-level jet in the average seasonal evolution (Fig.3b). The SST first decreases slightly in association with the expected convective cloud radiative forcing and the small wind perturbation and then remains relatively constant. After these first intraseasonal convective events, there is thus just a regulation of the

SST here instead of the cooling observed over northern Indian Ocean regions. These steady local conditions of SST and MLD for the whole monsoon season are in agreement with the observed relatively regular ISV.

Southern Indian Ocean and the Australian monsoon

The AROD is in December for the Western Indian Ocean and in January for the central Indian Ocean (Fig.2 and Table 1). Over Northern Australia, the AROD is in November and is thus sooner that the average onset date (25 December) given in Hendon and Liebmann (1990). This is due to the more equatorial position of our region that is indeed more characteristic of Timor and Arafura Seas than continental Australian regions over which the AROD is later (Fig.2). The SST remains nearly constant after the AROD and the low level jet associated to the monsoon-like circulation is weak and the MLD is small (Fig.3). The ISV of the OLR, the SST (Fig.3c) and the low-level wind (Fig.3d) is maximal between December and April, in association with the relatively small MLD (~30m). One may notice that over Northern Australia, the slight decrease of the ISV of the OLR in February-March (Fig.3c) corresponds to a slight increase of low-level wind and MLD (Fig.3b).

For these two regions, the intraseasonal events are not particularly strong nor particularly grouped near the AROD (Fig.3d and 4). Considering the composite of these events, the oscillation of the OLR is relatively marked (Fig.5), indicating also an average duration of about 30 days. In contrast with the other regions during the NH summer, the average decrease of the OLR after this first event is less important, in good agreement with the lower value of the AROI (Fig.2), especially over the Western Indian Ocean. Over Northern Australia, the wind increases and remains stronger after the intraseasonal event and the SST decreases slightly. Despite some similarities with the northern Indian Ocean region, the seasonal cycle of these two regions resembles more to that of South China Sea and Northwestern Pacific Ocean with a relatively even ISV throughout the season associated with an MLD of about 20-30 meters.

5. Summary and discussion

For different oceanic regions of the Indo-Pacific area, the average seasonal cycle of the ISV of the convection appears to be well related to the seasonal evolution of local SST and MLD. In addition, the average seasonal evolution of the MLD during summer months is forced by the low-level wind related to large-scale monsoon circulations. This relation between the ISV

of the convection and the seasonal monsoon march is particularly evident over the northern Indian Ocean regions. Strong and recurrent intraseasonal events are associated with the monsoon onset while the MLD is still shallow, giving statistically a large ISV in May for the Bay of Bengal and in June for the Arabian Sea. Just after the monsoon onset, the strong low-level monsoon jet deepens the mixed layer of these two oceanic regions. This reduces the reactivity of the mixed layer temperature to surface flux forcing and is consistent with a statistical reduction of the ISV of the convection during the core of the monsoon for these regions. Note that strong intraseasonal event may occasionally occur in the core of the monsoon season, such as in August 2000 over the Bay of Bengal (Vecchi and Harrison, 2002), may be in association with shallower MLD due to barrier layers (Shenoi et al, 2002). For the other considered monsoon regions, the low-level wind remains relatively small and the mixed layer relatively thin. For these regions, the ISV is more evenly distributed over the whole monsoon season, in agreement with the results of Maloney and Sobel (2004) showing that the convective ISV is maximal for an ocean mixed layer of about 20-30 m. One should note that the small ISV over continental India or continental Australia (Fig.1) is also in agreement with this result as far as soil can be compared to a very thin and reactive "mixed layer" or, more physically, to a "warm layer" with a large diurnal cycle of the surface temperature that rather tends to release the conditional instability every afternoon.

The study reported here did not consider the large-scale Indo-Pacific organisation of the intraseasonal convective perturbations. Even though large-scale organisation clearly impacts the pattern for particular events, one may question the necessity of such large-scale relation for the existence of some strong intraseasonal events over one single basin. For example, the local SST conditions linked to the seasonal cycle, such as over the northern Indian Ocean in May and June, increase the convective instability. In this case, one may suspect that any dynamical perturbation over the basin, such as those described by Lawrence and Webster (2002), is able to trigger strong convective events with an efficiency depending on the state of underlying oceanic surface including the MLD. Figure 1 clearly shows that the ISV is concentrated over northern Indian Ocean in May-June and over the northwestern Pacific in August, in good agreement with such a local effect of the surface conditions. While this is out the scope of this study, one may note that the existence of strong intraseasonal events over one single basin also questions the meaning of large-scale average ISV patterns. Goulet and Duvel (2000) showed that such an average indo-Pacific ISV pattern is indeed poorly representative of individual intraseasonal events for NH summer months. Duvel and Vialard

(2006) also found that, if ISV patterns for a given basin are well reproducible from one event to another, only few events well organized over one basin are also well organized over another basin of the Indo-Pacific area.

If the ISV amplitude is mainly driven by air-sea coupling, two main processes have to be considered. The first process is a local (basin-scale) convective instability induced by surface warming. This surface warming can be the result of the seasonal cycle or favoured by large-scale circulation partly driven by remote regions, as discussed in Annamalai and Sperber (2005). This warming may be enhanced by the formation of ocean warm layers if low-wind conditions prevail during the convectively suppressed phase. The second process is the negative feedback (regulating effect) of the convection on the SST through radiative flux and low-level wind response. Because of the induced cooling, this feedback could control in part the amplitude and the duration of the intraseasonal convective event. For the northern Indian Ocean region, this second process is strongly enhanced in June by the concomitant setting up of low-level monsoon jet. It is however difficult to say from the present analysis if the corresponding intraseasonal event is a cause or a consequence of the monsoon onset. This requires more detailed case studies. Also, the role of the MLD in different intraseasonal events has to be confirmed and analysed by further observational and modelling studies. This requires taking into account the basin-scale dynamical perturbations associated to the convection. The strong link between the Indian monsoon onset and the ISV of the convection reinforced the hypothesis that a correct representation of the ISV is necessary for a correct representation of the monsoon in coupled general circulation models. More generally, if the triggering and the duration of intraseasonal events are indeed mainly controlled by the ocean mixed layer heat content, a good representation of vertical structure of the upper ocean will be a necessary condition to correctly simulate and forecast the seasonal march of the monsoon rainfall, that includes its associated intraseasonal perturbations.

Acknowledgments: Hugo Bellenger was also supported by a Graduate Research Fellowship of Ecole Polytechnique. We thank A. Sobel and H. Annamalai for their very detailed and useful comments on a first version of this paper.

References

Annamalai, H., and K. R. Sperber, 2005: Regional heat sources and the active and break phases of boreal summer intraseasonal (30-50) variability, *J. Atmos. Sci.*, **62**, 2726-2748.

de Boyer Montégut, C., G. Madec, A. S. Fischer, A. Lazar, and D. Iudicone, 2004: Mixed layer depth over the global ocean: An examination of profile data and a profile-based climatology, *J. Geophys. Res*., **109**, C12003.

Duvel, J. P., R. Roca, and J. Vialard, 2004: Ocean mixed layer temperature variations induced by intraseasonal convective perturbations over the Indian Ocean, *J. Atmos. Sci.*, **61**, 1004-1023.

Duvel, J. P. and J. Vialard, 2006: Indo-Pacific Sea Surface Temperature Perturbations Associated with Intraseasonal Oscillation of the Tropical Convection, *J. Clim.*, (in press).

Fasullo, J. and P. J. Webster, 2003: A Hydrological Definition of Indian Monsoon Onset and Withdrawal, *J. Clim.*, **16**, 3200-3211.

Flatau, M. K., P. J. Flatau, and D. Rudnick, 2001: The dynamics of double Monsoon Onset, *J. Clim.*, **14**, 4130-4146.

Gill, A. E., 1980: Some simple solutions for heat-induced tropical circulation, *Quart. J. Roy. Meteor. Soc.*, **106**, 447-462.

Goulet, L., and J. P. Duvel, 2000: A new approach to detect and characterize intermittent atmospheric oscillations: Application to the intraseasonal oscillation, *J. Atmos. Sci.*, **57**, 2397-2416.

Harrison, D. E., and G. A. Vecchi, 2001: January 1999 Indian Ocean cooling event, *Geophys. Res. Lett.*, **28**, 3717-3720.

Hendon, H. H., and B. Liebmann, 1990: A composite study of onset of the Australian Summer Monsoon, *J. Atmos. Sci.*, **18**, 2227-2240.

Ho, L., and B. Wang, 2002: The time structure of the Asian-Pacific summer monsoon: a fast annual cycle view, *J. Clim.*, **15**, 2001-2019.

Inness, P. M., and J. M. Slingo, 2003: Simulation of the Madden–Julian Oscillation in a Coupled General Circulation Model. Part I: Comparison with Observations and an Atmosphere-Only GCM. *J. Climate*, **16**, 345–364.

Joseph, P. V., and S. Sijikumar, 2004: Intraseasonal variability of the low-level jet stream of the Asian summer monsoon, *J. Clim.*, **17**, 1449-1458.

Julian, P. R., 1971: Some aspects of variance spectra of synoptic scale tropospheric wind components in midlatitudes and in the tropics, *Mon. Wea. Rev.*, **99**, 954-965.

Kemball-Cook, S. and, B. Wang, 2001: Equatorial waves and air-sea interaction in the boreal summer intraseasonal oscillation, *J. Clim.*, **14**, 2923-2942.

Krishnamurthy, V. and, J. Shukla, 2000: Intraseasonal and interannual variability of rainfall over India, *J. Clim*., **13**, 4366-4377.

Lawrence, D.M., and P.J. Webster, 2002: The Boreal Summer Intraseasonal Oscillation: Relationship between Northward and Eastward Movement of Convection. *J. Atmos. Sci.*, **59**, 1593–1606

Maloney, E. D., and A. H. Sobel, 2004: Surface fluxes and ocean coupling in the tropical intraseasonal oscillation, *J. Clim.*, **17**, 4368-4386.

Reynolds, R. W., and T. M. Smith, 1994: Improved global sea surface temperature analyses using optimum interpolation, *J. Clim.*, **7**, 1195-1202.

Sengupta, D., and M. Ravichandran, 2001: Oscillations of Bay of Bengal sea surface temperature during the 1998 summer monsoon, *Geophys. Res. Lett.*, **28**, 2033-2036.

Shenoi, S. S. C., D. Shankar, and S. R. Shetye, 2002: Differences in heat budgets of near-surface Arabian Sea and Bay of Bengal: Implications for the summer monsoon. *J. Geophys. Res.*, 107 (C6), 3052, doi:10.1029/2000JC000679.

Sobel, A. H., and H. Gildor, 2003: A simple time-dependent model of SST hot spots. *J. Clim*., **16**, 3978-3992.

Stephens, G. L., P.J. Webster, R. H. Johnson, R. Engelen and T. L'Ecuyer, 2004: Observational Evidence for the Mutual Regulation of the Tropical Hydrological Cycle and Tropical Sea Surface Temperatures. *J. Clim.*, **17**, 2213-2224.

Vecchi, G. A., and D. E. Harrison, 2002: Monsoon breaks and subseasonal sea surface temperature variability in the Bay of Bengal, *J. Clim.*, **15**, 1485-1493.

Waliser, D. E., K. M. Lau, J.-H. Kim, 1999: The Influence of Coupled Sea Surface Temperatures on the Madden–Julian Oscillation: A Model Perturbation Experiment. *J. Atmos. Sci.*, **56**, 333–358.

Wang, B., and Q. Ding, 2006: Changes in global monsoon precipitation over the past 56 years, *Geophys. Res. Lett.*, **33**, L06711.

Wang, B., and L. Ho, 2002: Rainy season of the Asian-Pacific summer monsoon, *J. Clim.*,**15**, 386-398.

Wang, B., and X. Xu, 1997: Northern hemisphere summer monsoon singularities and climatological intraseasonal oscillation, *J. Clim.*, **10**, 1071-1085.

Zhang, C., and M. Dong, 2004: Seasonality in the Madden-Julian Oscillation, *J. Clim.*, **17**, 3169-3180.

Table 1: Number of strong intraseasonal convective events (amplitude larger than 40Wm^{-2} in the OLR filtered signal) for each region; average period of these strong events and the corresponding standard deviation (in days); average Rainfall Onset Date (AROD) and number of intraseasonal events at ±4 pentads from the AROD (events used for the composites of figure 5).

	Western Indian Ocean	Northern Australia	Arabian Sea	Northeast India	Bay of Bengal	South China Sea	Northwestern Pacific Ocean
Number of strong events	52	70	68	32	92	94	61
Average period and σ (days)	32±6	35±8	33±8	33±8	34±8	32±7	29±6
Average Rainfall Onset Date	15/12	19/11	28/05	12/06	03/05	13/05	12/07
Number of strong events at ±4 pentads from the AROD	13	14	20	12	21	17	12

Figure captions

Figure 1: Monthly mean standard deviation in the 20-90 day band for the OLR (Colours) and the module of the 850 hPa wind (contours solid: 3.5ms^{-1}; dashed: 2.5 ms^{-1}) given by NCEP re-analyses.

Figure 2: Average Rainfall Onset Date (AROD: colour in month) and Average Rainfall Onset Intensity (AROI: contour dotted for -5, dashed for -7.5 and solid for -12.5 Wm^{-2}pentad^{-1}) for the 1979-2004 OLR time series. Monsoon regions are delineated by the -5 Wm^{-2}pentad^{-1} contour in the AROI. Seven monsoon regions are selected and represented: Western Indian Ocean (WIO), Northern Australia (NA), Arabian Sea (AS), Northeast India (NI), Bay of Bengal (BoB), South China Sea (SCS) and the Northwestern Pacific Ocean (NPO).

Figure 3: Average regional seasonal cycle for (a) OLR (solid) and surface temperature (dashed); (b) 850 hPa wind speed (solid) and oceanic Mixed Layer Depth (MLD: dashed). Average standard deviation in the 20-90 day band for (c) OLR (solid) and surface temperature (dashed); (d) 850 hPa wind speed (dotted). Also represented in (d) is the number of strongest intraseasonal convective event per decade (bar). Black dots represent the Average Rainfall Onset Date (AROD; see also Table 1).

Figure 4: Seasonal distribution of the strongest convective events (circle) with open markers for the strong intraseasonal events located at ±4 pentads from the Average Rainfall Onset Date (AROD). The size of the circle is proportional to the amplitude (maximum minus the following minimum) of the events from 40 to 110 Wm^{-2}. The large stick shows the AROD for each region.

Figure 5: Composites of the raw pentad mean signals for the strongest intraseasonal convective events occurring at ±4 pentads from the Average Rainfall Onset Date (AROD) for the OLR (solid), the 850 hPa wind speed (dotted) and surface temperature (dashed). The origin of the composite time frame is the pentad of largest OLR decrease in the $\Re(\tilde{X}_f(t))$ signal.

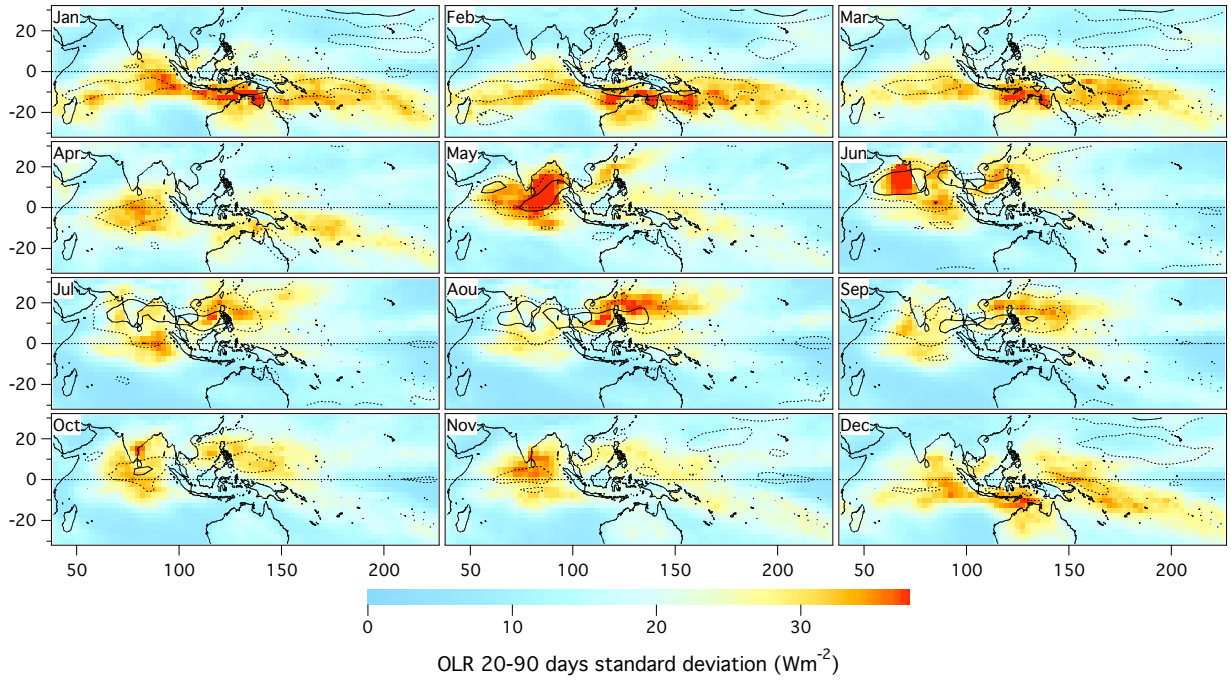

Figure 1: Monthly mean standard deviation in the 20-90 day bands for the OLR (Colours) and the module of the 850 hPa wind (contours solid: 3.5ms^{-1}; dashed: 2.5 ms^{-1}) given by NCEP re-analyses.

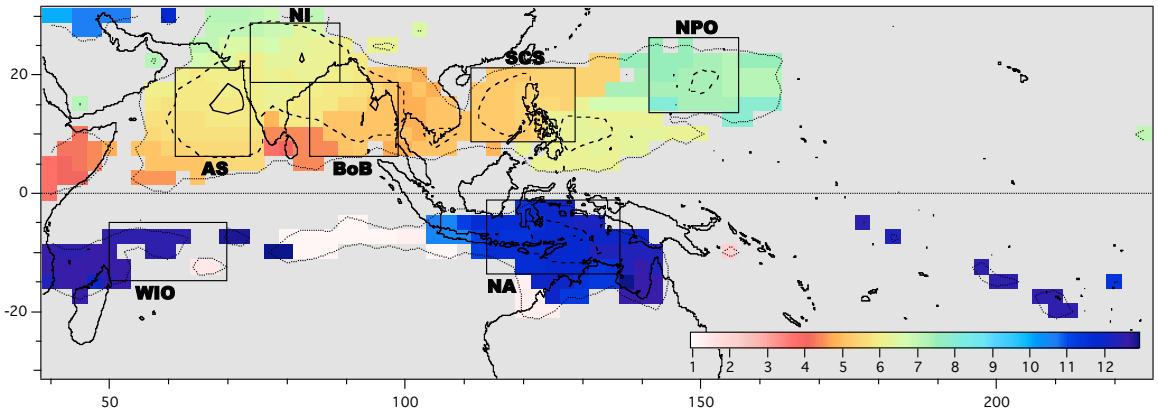

Figure 2: Average Rainfall Onset Date (AROD: colour in month) and Average Rainfall Onset Intensity (AROI: contour dotted for -5, dashed for -7.5 and solid for -12.5 $Wm^{-2}pentad^{-1}$) for the 1979-2004 OLR time series. Monsoon regions are delineated by the -5 $Wm^{-2}pentad^{-1}$ contour in the AROI. Seven monsoon regions are selected and represented: Western Indian Ocean (WIO), Northern Australia (NA), Arabian Sea (AS), Northeast India (NI), Bay of Bengal (BoB), South China Sea (SCS) and the Northwestern Pacific Ocean (NPO).

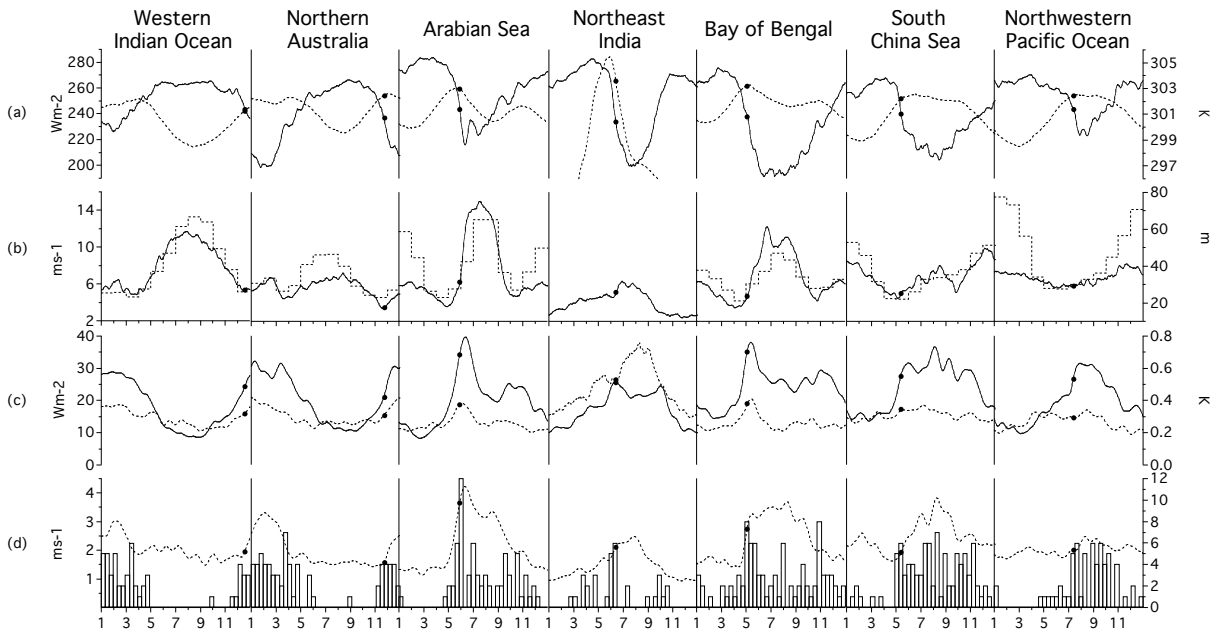

Figure 3: Average regional seasonal cycle for (a) OLR (solid) and surface temperature (dashed); (b) 850 hPa wind speed (solid) and oceanic Mixed Layer Depth (MLD: dashed). Average standard deviation in the 20-90 day band for (c) OLR (solid) and surface temperature (dashed); (d) 850hPa wind speed (dotted). Also represented in (d) is the number of strongest intraseasonal convective event per decade (bar). Black dots represent the Average Rainfall Onset Date (AROD; see also Table 1).

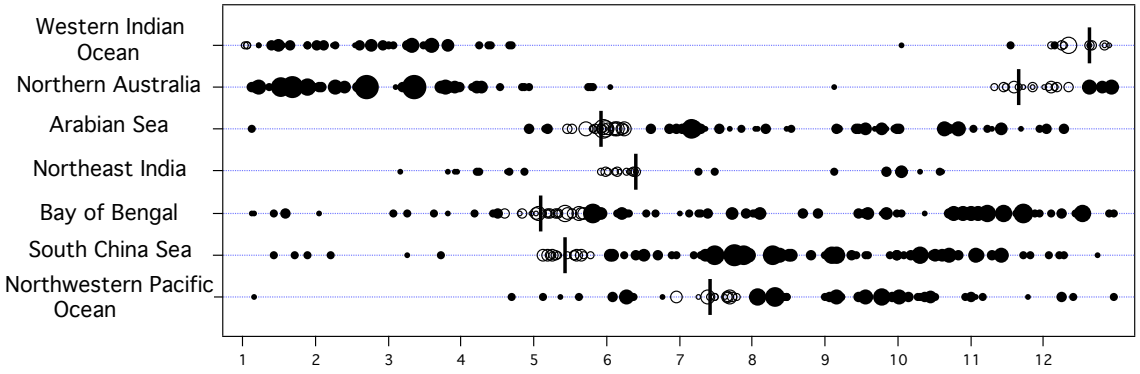

Figure 4: Seasonal distribution of the strongest convective events (circle) with open markers for the strong intraseasonal events located at ±4 pentads from the Average Rainfall Onset Date (AROD). The size of the circle is proportional to the amplitude (maximum minus the following minimum) of the events from 40 to 110 Wm^{-2}. The large stick shows the AROD for each region.

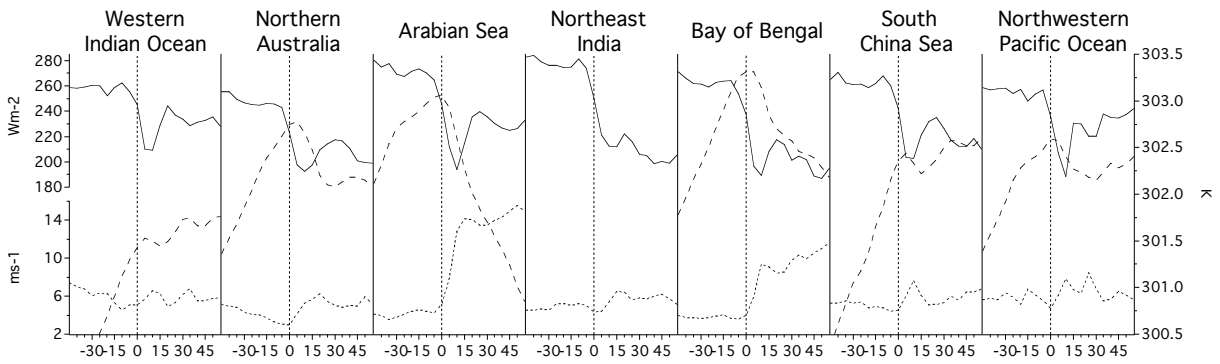

Figure 5: Composites of the raw pentad mean signals for the strongest intraseasonal convective events occurring at ±4 pentads from the Average Rainfall Onset Date (AROD) for the OLR (solid), the 850 hPa wind speed (dotted) and surface temperature (dashed). The origin of the composite time frame is the pentad of largest OLR decrease in the $\Re(\tilde{X}_f(t))$ signal.

of figure 5).